Reexamination of multiphoton ionization of xenon under 12.7-eV radiation

M. G. Makris[1] and P. Lambropoulos[1,2]

[1]*Institute of Electronic Structure and Laser, Foundation of Research and Technology Hellas, P. O. Box 1527, Herakleion 711 10, Crete, Greece*

[2]*Department of Physics, University of Crete, P. O. Box 2208, Herakleion 71003, Crete, Greece*

We present a theoretical analysis of multiphoton ionization of xenon pertaining to experimental data obtained by free electron laser (FEL) radiation of photon energy 12.7 eV by Wabnitz *et al.* [Phys. Rev. Lett. **94**, 023001 (2005)]. Taking also into consideration previous related theoretical information by Santra and Greene [Phys. Rev. A **70**, 053401 (2004)], we present a detailed study of the dependence of ionic yields on radiation intensity as well as the expected saturation intensities. Our emphasis is on the basic features characterizing such processes and in spite of analysis in terms of various scenarios, we find that some incompatibility between theory and experiment persists.

I. INTRODUCTION

This paper began as an attempt to reconcile presented experimental data [1] on multiphoton ionization of xenon by free electron laser (FEL) radiation of photon energy 12.7 eV on the one hand with a theoretical paper by Santra and Greene [2] and on the other hand with a new calculation using rate equations with scaled cross sections. It has been agreed that given the photon energy, and the range of intensities reached in the experiment, the processes involved fall within the validity of perturbation theory, and that is the basis of interpretation in Refs. [1,2]. Santra and Greene, however, did not produce laser power dependences for the various ionic species detected in the measurements. These power dependences and the resulting saturation intensities are very valuable in making contact with the data.

Our initial expectation was that no significant discrepancies would emerge, in which case, we would keep the results for our internal use in calibrating our approach, as we have embarked on similar calculations [3] for much shorter wavelengths and higher intensities, for which experimental data have began appearing some time ago [4]. To our surprise, that was not the case. A number of discrepancies between theory and experiment seem to emerge. Thus, our purpose here is to present and discuss those discrepancies, in the hope that they can eventually be resolved, or at least kept in mind, since the experiment was completed and closed some time ago and was in fact the first of its kind using FEL radiation.

Although, given the pulse duration τ and the cross section σ leading to a particular species through an N-photon process, the order of magnitude of the saturation intensity $F(s)$ can be obtained through the relation $F^N \sigma \tau \sim 1$, for a quantitative answer, one needs to solve the kinetic differential equations governing the evolution of the species during the pulse. In addition, the slope of the radiation power dependence of a species, produced through N-photon ionization even within perturbation theory, is expected to be N only as long as the initial species population is essentially constant and the final species not depleted substantially, which is not necessarily the case in the presence of a sequence of ionization events. Otherwise, the slopes expected to be found in an

experiment can only be predicted and/or interpreted through the solution of the kinetic equations. Finally, the intensity fluctuations, inevitably present, at least in this stage of development of the free electron laser in Hamburg (FLASH), need to be folded in, an issue that has been addressed by Santra and Greene. Such intensity fluctuations and their effect on multiphoton processes have been studied in great detail over the last 25 years. In the present context, we have a rather simple case since no strongly driven bound-bound transitions are involved. What is known from past experience is that, for a truly chaotic radiation field, an N-photon transition into a continuum, such as ionization, is enhanced by a factor of $N!$ [5,6], as if the effective multiphoton cross section were larger. Again, exactly how this effect is manifested in a particular experiment, will come out of the kinetic equations.

II. CROSS SECTIONS AND CALCULATIONS

We consider the sequential ionization of the different Xe species, up to Xe^{5+}, in the lowest order of perturbation theory available for each step. This leads us to the following set of equations for the populations of each species:

$$\dot{N}_0 = - \sigma_{01}^{(1)} F(t) N_0,$$

$$\dot{N}_1 = \sigma_{01}^{(1)} F(t) N_0 - \sigma_{12}^{(2)} F^2(t) N_1,$$

$$\dot{N}_2 = \sigma_{12}^{(2)} F^2(t) N_1 - \sigma_{23}^{(3)} F^3(t) N_2,$$

$$\dot{N}_3 = \sigma_{23}^{(3)} F^3(t) N_2 - \sigma_{34}^{(4)} F^4(t) N_3,$$

$$\dot{N}_4 = \sigma_{34}^{(4)} F^4(t) N_3 - \sigma_{45}^{(5)} F^5(t) N_4,$$

$$\dot{N}_5 = \sigma_{45}^{(5)} F^5(t) N_3 - \sigma_{56}^{(6)} F^6(t) N_5,$$

$$\dot{N}_6 = \sigma_{56}^{(6)} F^6(t) N_5,$$

where N_0 and $N_{i=1-5}$ stand for the population of neutral Xe and the first five ionized species, $F(t)$ for the photon flux of

TABLE I. Cross sections and saturation intensities for the first six Xe ions. In the first column, n stands for the ionization stage of Xe and the following two columns give the cross section for the sequential ionization process $Xe^{(n-1)+} \rightarrow Xe^{n+}$ with a photon energy $\simeq 12.7$, as reported in Ref. [2] and as obtained by scaling. In the columns that follow, we give the estimated saturation intensity from the cross sections of Ref. [2] (see text for details), the saturation intensity from the experiment of Wabnitz *et al.*, and the estimated values for the cross sections that follow from the experimental data. In the final column we show the cross-section values employed in Fig. 3. Cross sections are given in $cm^{2n} s^{n-1}$ and saturation intensities in W/cm^2. In the third column, the single photon cross section inside parentheses is scaled to obtain the rest of the cross sections.

n	CS (Ref. [2])	CS (scaling)	P_s (estimated)	P_s (Ref. [1])	CS (estimated)	CS (Fig. 3)
1	119×10^{-18}	(119×10^{-18})	1.6×10^{11}			40×10^{-18}
2	4.6×10^{-49}	3.4×10^{-49}	7.7×10^{12}			2.5×10^{-46}
3	2×10^{-82}	4×10^{-81}	4.8×10^{13}	$(5 \pm 3) \times 10^{12}$	$3 \times 10^{-78} - 4 \times 10^{-80}$	1.8×10^{-79}
4	3.3×10^{-115}	1×10^{-113}	7.8×10^{13}	$(9 \pm 6) \times 10^{12}$	$2 \times 10^{-109} - 3 \times 10^{-112}$	2.1×10^{-111}
5	3.7×10^{-147}	2.2×10^{-147}	7.0×10^{13}	$>10^{13}$	$<6 \times 10^{-143}$	8.3×10^{-147}
6	6.4×10^{-179}	1×10^{-180}	5.7×10^{13}			6.4×10^{-179}

the FEL pulse and σ the cross sections for the respective processes. The superscript in the cross sections denotes the order of the process and the subscript stands for the initial and final species. We neglect any potential contribution from the harmonics of the FEL.

The cross sections for these processes were calculated in Ref. [2]. Due to the lack of any other calculations for these cross sections, we also estimated their value based on the scaling of the single photon ionization cross section of Xe, an approach explained in more detail in [3,7]. The value of $\sigma_{01}^{(1)}$ as reported in Ref. [1] is around 40 Mb, while its value at photon energy 13.4 eV is 65 Mb [8,9]. In any case, for pulse duration around 50 fs, $\sigma_{01}^{(1)}$ is large enough to lead to saturation of Xe^+ production at intensities around 10^{11} W/cm^2, i.e., at intensity much lower than the intensity range of interest here. Since we want to have a direct comparison of our scaling approach with the cross section calculation of Ref. [2], we will employ the calculated value [2] of $\sigma_{01}^{(1)} = 119$ Mb, keeping in mind that we will arrive at rather generous values for the cross sections. For the low order cross sections, we followed our approach described in detail in Ref. [3], employing the available two-, three-, and four-photon single ionization calculated cross sections of the He atom, as a scaling prototype [10,11]. For the higher order cross sections, i.e., $\sigma_{45}^{(5)}$ and $\sigma_{56}^{(6)}$, we proceeded as in [7]. The cross sections we arrive at are shown in Table I and are in good agreement with those calculated in Ref. [2], in the sense that the values of $(\sigma^{(n)})^{1/n}$ are comparable. This comparison represents a redundancy test in that two significantly different methods produce practically similar results for the cross sections.

For the FEL laser temporal shape, we consider either a simple Gaussian with full width at half-maximum (FWHM) $\tau = 100$ fs as reported in the experiment, or a pulse with amplitude fluctuations, resembling the pulses obtained by simulations of the FEL laser [2,12,13], in which case it is the average of the FEL pulses that tends to a Gaussian with FWHM τ. The amplitude-fluctuating FEL pulse is constructed as follows: Each pulse consists of a superposition of a few Gaussian (5 in the present paper) with the FWHM of each Gaussian randomly distributed from $\tau/10$ to $\tau/4$. The center of each Gaussian is normally distributed with a width equal to τ. The intensity of each Gaussian is randomly chosen in between 0.1 and 3 times the maximum intensity of the pulse. The total energy of the pulse is kept constant by a final normalization of the intensities of each Gaussian. The average of the FEL pulses constructed this way is very close to a Gaussian with FWHM τ.

The spatial profile of the FEL beam perpendicular to the axis is a Gaussian with an intensity profile near the focus ($z=0$) as in Ref. [2], i.e.,

$$I(\rho, z) = \frac{1}{1 + (z/z_0)^2} \exp\left(-\frac{4 \ln 2}{\pi \Delta^2(z)} \rho^2\right) I_0, \quad (1)$$

$$\Delta(z) = \Delta \sqrt{1 + (z/z_0)^2}, \quad (2)$$

where Δ is the FWHM (z-dependent) of the beam profile and I_0 is the maximum intensity at the focus of the FEL. Since we are interested in obtaining results that can be directly compared to the experiment, we must include in our calculations the focusing conditions and the detector specifications. Thus, in accordance with Refs. [1,2] we set $\Delta = 20$ μm, $z_0 = 1.2$ mm and center the detector at the focus of the FEL with an acceptance window of 2 mm along the beam direction.

The differential equations for the populations are solved for a dense enough set of intensity values, ranging from zero to the maximum value we consider and the final population of each species [$N_i(I)$, where i stands for the xenon species] is interpolated after the laser pulse is over. It is now straightforward to perform the space integral in the laser focus to obtain the space averaged ion production P_i for each species,

$$P_i = \int_0^{\rho_{max}} \int_{z_{min}}^{z_{max}} 2\pi \rho N_i(I(\rho, z)) dz d\rho. \quad (3)$$

TABLE II. In the first line of the table we give the expected ion signal for an FEL laser pulse of 50 fs and energy of the order of 10 μJ from the simulations of Ref. [2]. In the two following lines we give our results, by employing the same focusing conditions and cross sections, with a Gaussian pulse envelope. In the last two lines, the cross sections are multiplied by $N!$ to represent effectively a completely chaotic FEL pulse. The maximum intensity of the pulse in Ref. [2] is about 5×10^{13} W/cm^2, and $\sigma_{01}^{(1)}=50$ Mb [14].

Intensity (W/cm^2)	Xe$^+$	Xe^{2+}	Xe^{3+}	Xe^{4+}	Xe^{5+}	Xe^{6+}
5×10^{13}	1×10^8	4.6×10^7	3.2×10^6	1.2×10^5	1.2×10^4	3.5×10^3
5×10^{13}	$1.\times10^8$	3.8×10^7	0.4×10^6	2×10^2	0	0
1×10^{14}	$1.\times10^8$	5.6×10^7	3.6×10^6	2.7×10^4	10^2	0.4
5×10^{13}	9.4×10^7	4.6×10^7	2.6×10^6	3×10^4	4.3×10^2	1.6×10^1
7×10^{13}	9.4×10^7	5.22×10^7	6.5×10^6	2.5×10^5	1.6×10^4	4.4×10^3

III. RESULTS

To begin, we would like to compare our results with those of Ref. [2]. We employ the same focusing conditions, pulse duration, and a Gaussian for the FEL envelope. Since a Gaussian cannot account for the fluctuations of the FEL intensity, the upper limit of the ionization enhancement expected can be taken into account by incorporating into the respective cross sections an order-dependent factor, which we take to be the one for a completely chaotic field, i.e., $N!$. The maximum pulse intensity at the FEL focus with the conditions of Ref. [2], for a total pulse energy of the order of 10 μJ, is of the order of 5×10^{13} W/cm^2.

In Table II we present the ionization yield from a Gaussian with FWHM 50 fs, with the cross sections of Ref. [2] and with the $N!$ enhancement for comparison. With a Gaussian pulse envelope, the ion signal we obtain is much lower for the ions higher than Xe^{2+} for this intensity, and even an increase of the intensity up to 10^{14} W/cm^2 does not lead to high enough ion yield for Xe^{5+} and Xe^{6+} compared with the calculations of Ref. [2]. Incorporating a $N!$ factor in the cross sections, leads to the ionization yield expected from a chaotic laser field. We give the ionization yield for two values of the maximum intensity of the FEL pulse, to stress the intensity sensitivity of the ionization in this intensity range. These intensities, i.e., 5×10^{13} and 7×10^{13} W/cm^2 correspond to pulses of total energy 10 and 14 μJ, respectively. With FEL intensity 5×10^{13} W/cm^2, ion yields up to Xe^{4+} are compatible with those reported in Ref. [2], but the yields of Xe^{5+} and Xe^{6+} are substantially lower. With FEL intensity 7×10^{13} W/cm^2, the yields of all species are compatible with those of Ref. [2]. Note that a factor of 2 difference in the ion yield, between a Gaussian pulse with FWHM 50 fs, with cross sections to account for a completely chaotic field, and on the other hand pulses that come out from a simulation [13] and average to a pulse of FWHM 50 fs, is well justified.

We are mainly interested in the power dependence of the ionization of the different xenon species, and since the actual temporal structure of the FEL pulse remains unknown, an estimate of its potential influence on the power dependence is valuable. To this end we calculate the intensity dependent production of the different xenon species employing both a smooth Gaussian pulse envelope, and a fluctuating envelope as described in the preceding section. For the latter, since it is constructed randomly, we take the average of 20 different pulses.

Employing the cross sections suggested in Ref. [2] again, we calculate the power dependence of the xenon species population, with the results shown in Fig. 1. As expected (Refs. [5,6]), the difference in the ionization between a Gaussian pulse and one with a fluctuating envelope increases with the order of the process. For Xe$^+$, which is produced via a first-order process, the ionization power dependence is essentially the same, affected only by the two photon ionization of Xe$^+$, once it sets in. In higher species, that are produced by multiphoton absorption, a displacement toward lower intensities, in the power dependencies of the population in the $\log_{10}-\log_{10}$ scale of Fig. 1, for the fluctuating versus the Gaussian FEL pulse, is evident. This displacement gradually reaches up to a factor of (slightly less than) 2 for Xe^{5+}, essentially leaving unaffected the slope of the population power dependence. We note here that for a truly chaotic laser field, the displacement of Xe^{5+} would be a factor of $(5!)^{1/5} \simeq 2.6$ pointing to the fact that the random pulse, as we constructed it, does not quite represent a chaotic field. Other minor modifications, at intensities around or above saturation can be attributed to the nonuniform shift of the saturation intensities of the other species. We can thus conclude that the pulse envelope structure does not influence the slopes of the
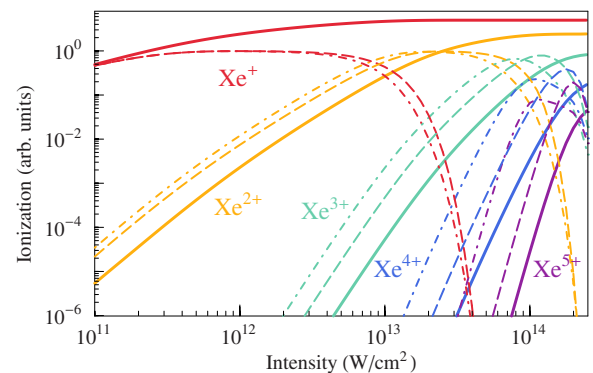

FIG. 1. (Color online) Ionization of Xe atoms with cross sections taken from [2] and the FEL laser pulse envelope being a Gaussian (dashed line) or a fluctuating pulse (dotted-dashed line). For the latter we show the average of 20 different pulses. Together we show the space averaged ion production in the laser focus (heavy line) assuming a Gaussian envelope, calibrated with Xe$^+$ production at low intensities. The correspondence between colors and species is the same for all figures.
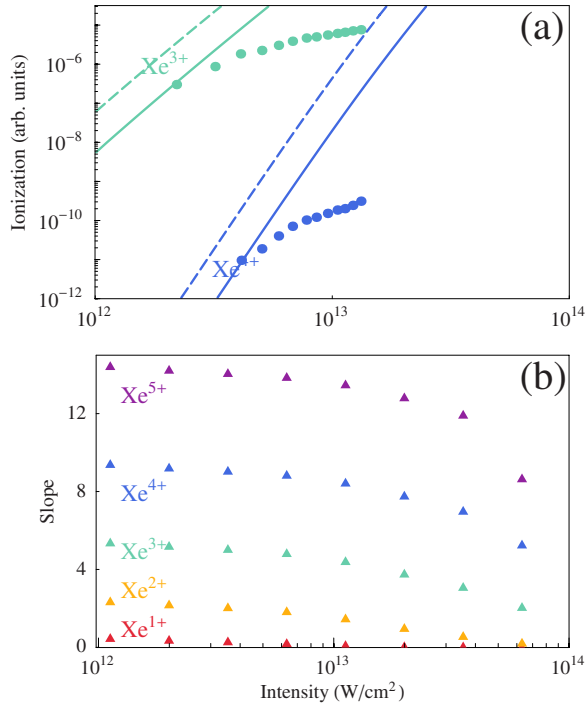
FIG. 2. (Color online) (a) Single atom (dashed line) and space averaged (continuous line) ionization yields of Xe^{3+} and Xe^{4+} with focusing conditions and detector characteristics as reported in Refs. [1,2] and the FEL pulse envelope Gaussian. The cross sections are those of Ref. [2] multiplied by $N!$. Space averaged ion production is calibrated with Xe^+ production at low intensities and the experimental data of Ref. [1] are displaced vertically to match the calculations. (b) Slope of (space averaged) ion production for the first five xenon species with parameters as in (a).

different species and thus in the following we will assume a Gaussian envelope for the FEL pulse. The ionization enhancement due to the pulse fluctuations will be taken into account by multiplying the cross sections with the respective $N!$.

In the experiment of Ref. [1], the slopes of the Xe^{3+}, Xe^{4+}, and Xe^{5+} production are reported to be equal to the order of the sequential process that leads to each species. Before proceeding, let us discuss the expected slope. In general, in a sequential process, one would expect the population of Xe^{i+} to exhibit a slope equal to the order of the process that ionizes $Xe^{(i-1)+}$, only in the intensity range that meets the following conditions: First, the population of $Xe^{(i-1)+}$ should be effectively constant, and second, the ionization of Xe^{i+} to $Xe^{(i+1)+}$ is not substantial. If either of these conditions is not fulfilled, the slope cannot be assumed to be predicted simply by the order of the process.

The power dependencies and the slopes of the (space averaged) Xe^{3+} and Xe^{4+} population, employing again the calculated cross sections and the experimental conditions of [1,2], are shown in Fig. 2. The experimental data do not match the space averaged ion population expected from our simulations. In more detail, with laser intensity around 3×10^{12} W/cm² i.e., close to the center of the intensity range employed in the experiment, to extract the slope, Xe^{3+} pro-

duction exhibits a slope of a bit more than 5 versus the reported 2.9 ± 0.2. This difference, of the calculated slope from the order of the sequential process that produces Xe^{3+} from Xe^{2+}, is due to the increase in the same intensity range of the Xe^{2+} population with slope of 2, since the Xe^+ is practically saturated at this intensity. A similar situation is encountered for Xe^{4+} at laser intensity 6×10^{12} W/cm², where the slope that comes out of the calculations is 9, i.e., the sum of the expected slopes of the sequential production of Xe^{2+}, Xe^{3+}, and Xe^{4+}.

In order to trace in more detail the reason for the discrepancy between our calculations and the experiment, we estimate the saturation intensity for each species. Assuming that $Xe^{(i-1)+}$ is already saturated and that depletion of Xe^{i+} is not significant, the saturation intensity for Xe^{i+} is given by the equation

$$1 = \int_t \sigma^k F^k(t)dt, \tag{4}$$

where k is the order of the process leading from $Xe^{(i-1)+}$ to Xe^{i+} and $F(t)=I(t)/\hbar\omega$ is the photon flux. These conditions can be checked *a posteriori*, by comparing the saturation intensities of the different species, but in any case, this simple equation gives a good estimate of the expected saturation intensity. The saturation intensity of a chaotic laser field is evidently smaller by a factor of $N!^{1/N}$. To be on the safe side, the saturation intensities of Table I are calculated with the assumption of a completely chaotic FEL pulse, and can thus be considered as the low limit of the actual saturation intensity.

The saturation intensity of Xe^{2+} is around 8×10^{12} W/cm², which means that it is not saturated in the intensity region where the slopes were extracted in the experimental paper [1]. For Xe^{3+} and Xe^{4+}, the saturation intensities are estimated to be a bit less than one order of magnitude above the ones reported in the experiment. Although the two theories obtain similar values for the cross sections, as described in Sec. II, the experimental results seem incompatible with those values.

As a way of examining the degree of discrepancy between theory and experiment, we consider now a reverse approach, in which we seek cross sections compatible with the data. We will focus on Xe^{3+} and Xe^{4+}, the only species for which intensity dependencies have been given in Ref. [1]. To be precise, the very limited data on the intensity dependence of Xe^{5+} of Ref. [1] are not a useful basis for comparison with theory. To this end, the cross section for Xe ionization is now taken from experimental data (Refs. [8,9]) to be around 40 Mb and the cross section for Xe^+ is assigned intentionally a large value, so that the Xe^{2+} population is saturated at intensities lower than 10^{12} W/cm², i.e., optimum conditions for the observation of a slope of 3 for Xe^{3+} production. The cross sections for Xe^{3+} and Xe^{4+} are estimated from the reported saturation intensities to be $\sigma_{23}^{(3)}=1.8 \times 10^{-79}$ cm⁶ s², $\sigma_{34}^{(4)}=2.1 \times 10^{-111}$ cm⁸ s³, respectively. The saturation intensity for Xe^{5+} appears to be outside the intensity range of the experiment, leaving us the option to choose a value that would not interfere with the slope of Xe^{4+}, i.e., a cross sec-
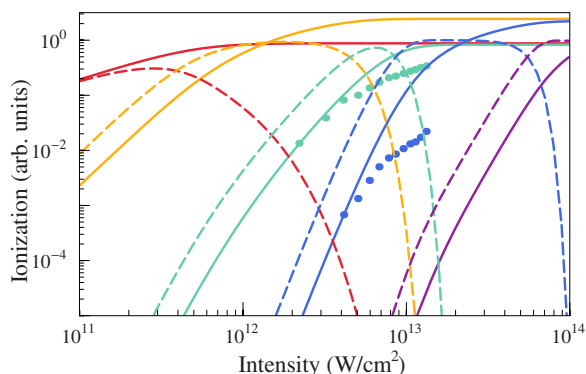
FIG. 3. (Color online) Ionization of xenon atoms (dashed line) and the expected detector signal for the first five xenon ion species, with cross sections of the last column of Table I. Experimental data are displaced vertically to match the calculations.

tion that would lead to a saturation intensity significantly higher than the saturation intensity of Xe^{4+}. To be on the safe side again, we choose the value $8.3 \times 10^{-147} cm^{10} s^4$ for $\sigma_{45}^{(5)}$, leading to a saturation intensity of 6×10^{13} W/cm^2, that would not modify the slope of Xe^{4+} in the intensity range of the experiment. Cross sections for the production of ions higher than Xe^{5+} do not interfere with the power dependence of the populations of Xe^{3+} and Xe^{4+}, since the atom ionization is sequential. We thus adopt the value for $\sigma_{56}^{(6)}$ suggested in Ref. [2], for completeness. We note here again that any increase of ionization due to the pulse structure is effectively considered as an $N!$ multiplying the respective cross section.

In Fig. 3, we show the signal for the Xe species along with the experimental data for Xe^{3+} and Xe^{4+} with the new set of cross sections. For Xe^{3+}, our calculations and the experimental data exhibit approximately the same slope for low intensities, i.e., before saturation, but for higher intensities there is a clear difference of up to a factor of 2 at 10^{13} W/cm^2. On the other hand, the slope of Xe^{4+} in the simulations is around 6, which does not match the experiment. We employed a range of values, for $\sigma_{34}^{(4)}$, but we were still unable to obtain results compatible with the power dependence of the experiment. This happens despite the fact that we carefully selected the relevant cross sections, so that the conditions, as far as cross sections are concerned, are (artificially) optimum for deriving slopes similar with the experiment.

We attribute this discrepancy to the proximity of the saturation intensities of Xe^{3+} and Xe^{4+} reported in Ref. [1]. This implies, that the population of Xe^{3+} cannot be considered as constant and thus the slope of Xe^{4+} cannot be expected to be equal to the order of the process $Xe^{3+} \rightarrow Xe^{4+}$.

We note again that the pulse envelope structure does not influence the slopes, and its detailed form would be important, only if high accuracy values for the cross sections (especially the high order ones) were to be obtained from the experimental data. Otherwise, any increase of the ionization signal due to envelope fluctuations can be considered as incorporated in the cross-section value.

In closing this section, one further process not included in our analysis should perhaps be given some consideration;

namely, the possibility of two-electron excitations in xenon. In fact, such excitations, which can be of importance in two-electron atoms such as the alkaline earths, have on occasion been found to play some role even in rare gases [15]; albeit at a significantly different wavelength range. The most likely mechanism in such cases has been the excitation of an outer $(5p)$ electron, accompanied by the excitation of a $(5s)$, from the subshell immediately below. This has to do with the structural fact that the first excited state of Xe^+ involves the excitation of a $(5s)$ rather than a $(5p)$ electron. Having pondered such a possibility in the present case, we found no plausible scenario for the involvement of such channels, within the wavelength range under consideration. The signature of a process of this type would appear as an inflection in the radiation power dependence of the yield for Xe^{2+}, for which there are no data.

IV. CONCLUDING REMARKS

Our attempt to reconcile presented experimental data on multiphoton multiple ionization of xenon by xuv radiation with a theoretical analysis, including all necessary ingredients has uncovered certain discrepancies. On the other hand, our findings are basically compatible with previous theoretical considerations

Several facets of the ingredients that went into our analysis have been presented and discussed exhaustively in the preceding sections. Two aspects, necessary for a quantitative contact with the data, have been included in our analysis; namely, the dependence of ionic yields on laser intensity and the respective saturation intensities. The two are related, because the saturation intensity for a particular ionic species can be read off the plot of the intensity dependence of the species; except for extremely unusual circumstances of no relevance to this case. Within the relevant experimental error bars, it is the value of the intensity at which the curve of the intensity dependence begins "bending over," by which we mean changing to lower slope. Theoretically, this value can be inferred and/or predicted, in terms of the relevant cross section and the pulse duration, as already discussed in this paper. A disagreement with experimental data, could be attributed to a wrong value of the cross section. Field intensity fluctuations can also affect the result, since their presence appears as an enhanced cross section. That is why in our analysis here we have considered a number of scenarios.

The slopes of the intensity dependence curves, however, provide a more stringent test. They are not affected directly by field fluctuations, while their dependence on the cross sections is less direct. Again, by examining various scenarios in terms of cross sections and field fluctuations, we have endeavored to avoid the influence of one particular parameter.

As is evident from the results of our analysis and in particular Figs. 2 and 3, it does not seem possible to obtain the experimental slopes for Xe^{3+} and Xe^{4+} theoretically, with the exception of Xe^{3+} in Fig. 3 which however is based on a calculation with cross sections hand picked to match the data as much as possible. In case it needs repeating, the same disagreement emerges if one uses the theoretical cross sec-

tions of Ref. [2], as demonstrated in Fig. 2. On the other hand, the systematic behavior of the theoretical intensity dependences shown in Figs. 1–3, is consistent with expectations based on the long history of multiphoton ionization over the last 40 years. At this point, 2 years after the experiment was completed, it would not be meaningful or useful to speculate on the reasons for these discrepancies. After all, this having been one of the experiments with a source of a new type, uncontrollable uncertainties on the intensity and the interaction region would not be too surprising. We believe, however, that it is useful to keep them in mind, in view of the new generation of data that are expected to follow.

[1] H. Wabnitz, A. R. B. de Castro, P. Gürtler, T. Laarmann, W. Laasch, J. Schulz, and T. Möller, Phys. Rev. Lett. **94**, 023001 (2005).

[2] R. Santra and C. H. Greene, Phys. Rev. A **70**, 053401 (2004).

[3] M. G. Makris and P. Lambropoulos, Phys. Rev. A **77**, 023401 (2008).

[4] A. A. Sorokin, M. Wellhofer, S. V. Bobashev, K. Tiedtke, and M. Richter, Phys. Rev. A **75**, 051402(R) (2007).

[5] C. Lecompte, G. Mainfray, C. Manus, and F. Sanchez, Phys. Rev. A **11**, 1009 (1975).

[6] P. Lambropoulos, Adv. At. Mol. Phys. **12**, 87 (1976).

[7] P. Lambropoulos and X. Tang, J. Opt. Soc. Am. B **4**, 821 (1987).

[8] J. West and J. Morton, At. Data Nucl. Data Tables **22**, 103 (1978).

[9] J. Samson and W. Stolte, J. Electron Spectrosc. Relat. Phenom. **123**, 265 (2002).

[10] A. Saenz and P. Lambropoulos, J. Phys. B **32**, 5629 (1999).

[11] L. A. A. Nikolopoulos and P. Lambropoulos, J. Phys. B **34**, 545 (2001).

[12] W. Ackermann *et al.*, Nat. Photonics **1**, 336 (2007).

[13] M. Dohlus, K. Flöttmann, O. S. Kozlov, T. Limberg, P. Piot, E. L. Saldin, E. A. Schneidmiller, and M. V. Yurkov, Nucl. Instrum. Methods Phys. Res. A **530**, 217 (2004).

[14] R. Santra (private communication).

[15] D. Charalambidis, P. Lambropoulos, H. Schröder, O. Faucher, H. Xu, M. Wagner, and C. Fotakis, Phys. Rev. A **50**, R2822 (1994).